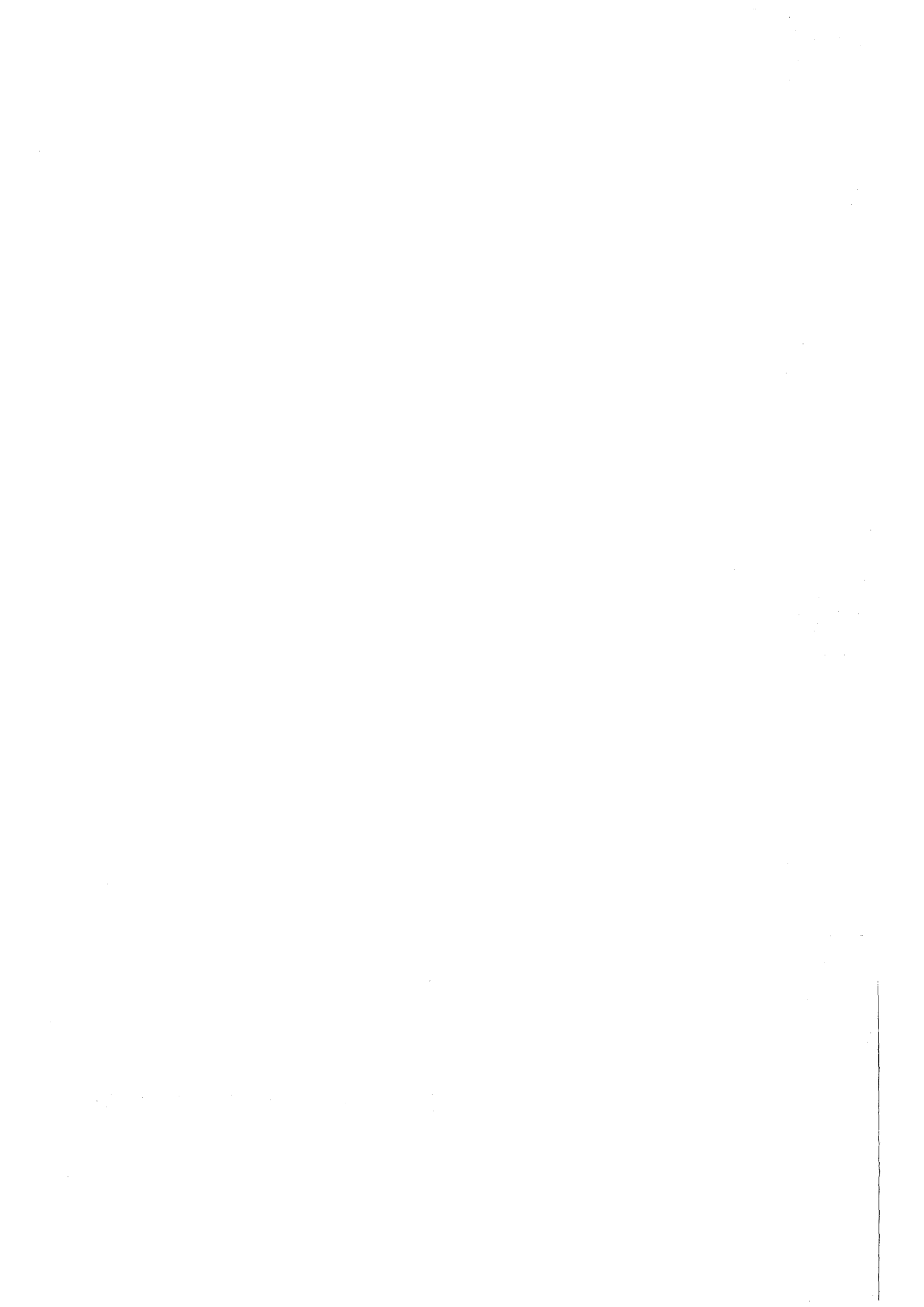


KfK 4110
Juli 1986

Recent Results on New Particle Searches at PETRA

H. Küster
Institut für Kernphysik

Kernforschungszentrum Karlsruhe



KERNFORSCHUNGSZENTRUM KARLSRUHE

Institut für Kernphysik

KfK 4110

RECENT RESULTS ON
NEW PARTICLE SEARCHES AT PETRA ¹

HERMANN KÜSTER ²

Kernforschungszentrum Karlsruhe GmbH, Karlsruhe

¹Invited talk at the XXI. Rencontre de Moriond on *Perspectives in Electroweak Interactions and Unified Theories*, Les Arcs, March 9-16 1986

²Mailing address: DESY F36, Notkestraße 85, 2000 Hamburg 52, F.R. Germany
Bitnet address: user F36HKU at node DHHDESY3

Als Manuskript vervielfältigt
Für diesen Bericht behalten wir uns alle Rechte vor

Kernforschungszentrum Karlsruhe GmbH
Postfach 3640, 7500 Karlsruhe 1

ISSN 0303-4003

RECENT RESULTS ON NEW PARTICLE SEARCHES AT PETRA

Abstract

Recent searches for new particles at PETRA are reviewed. Results on heavy lepton searches (charged and neutral), supersymmetry searches (SUSY partners of the electron, the photon, the W and Z gauge bosons, and the Higgs), and on searches for compositeness (excited leptons and leptoquarks) are presented.

NEUE ERGEBNISSE ZUR SUCHE NACH NEUEN TEILCHEN BEI PETRA

Zusammenfassung

Neue Ergebnisse zur Suche nach neuen Teilchen werden diskutiert. Ergebnisse zur Suche nach schweren Leptonen (geladen und neutral), zur Suche nach Supersymmetrie (SUSY Partner des Elektrons, des Photons, der W und Z Eichbosonen und der Higgs Teilchen), und zur Suche nach Substrukturen (angeregte Leptonen und Leptoquarks) werden vorgestellt.

1 Introduction

The Standard Model of electroweak and strong interactions gives a very simple and elegant view of the spectrum of fundamental particles and their interactions. Although at present it describes all experimental observations with remarkable accuracy it leaves many fundamental questions unanswered:

- what determines the quark and lepton mass spectrum ?
- why are there at least 3 repetitive fermion families ?
- a fundamental theory should unify all interactions, including gravity
- what stabilizes the Higgs mass with respect to radiative corrections ?

This partial list illustrates the need to beyond the Standard Model. Prominent candidates for such a theory are compositeness where part or all of the Standard Model particles are thought to be composite particles and supersymmetry which proposes a symmetry between bosons and fermions by introducing a fermionic partner for each boson and vice versa. Unambiguous guidelines on the way beyond the Standard Model can only come from the finding or non finding of new particles not accounted for by the Standard Model.

High energy e^+e^- collisions are a good place to look for the production of new particles. Before discussing specific searches I would like to make some general remarks on new particle production mechanisms in e^+e^- collisions. The most simple case is the pair production of charged particles via single photon annihilation (Fig. 1a). The cross section depends on charge, spin, and mass of the particle:

$$\sigma(e^+e^- \rightarrow X^+X^-) = Q^2 \frac{\beta(3-\beta^2)}{2} \sigma_{\mu\mu} \quad \text{for spin } 1/2$$

$$\sigma(e^+e^- \rightarrow X^+X^-) = Q^2 \frac{1}{4} \beta^3 \sigma_{\mu\mu} \quad \text{for spin } 0$$

Here $\sigma_{\mu\mu}$ stands for the lowest order QED μ pair cross section. Fig. 2 illustrates the threshold behavior for pair production of spin 0 and spin 1/2 particles. In the spin 0 case the cross section is suppressed

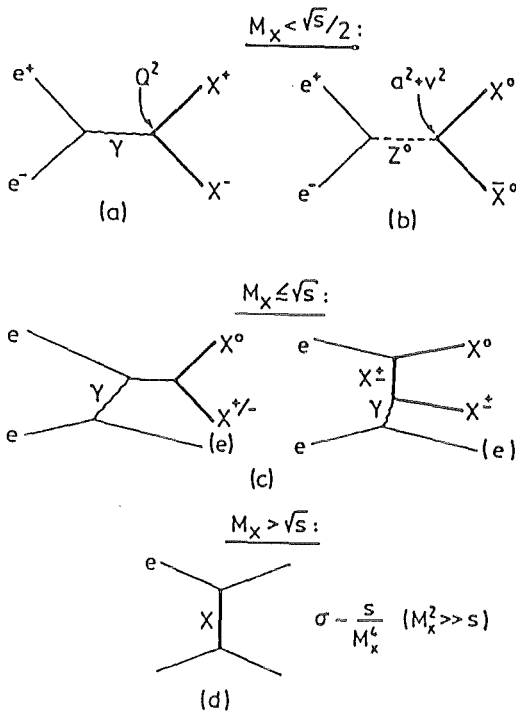


Figure 1: New particle production processes in e^+e^- collisions.

(a): pair production of a charged particle (e.g. $e^+e^- \rightarrow L^+L^-$)

(b): pair production of a neutral particle via virtual Z^0 exchange (e.g. $e^+e^- \rightarrow N\bar{N}$)

(c): single production of a charged particle together with a neutral one in $e\gamma$ collisions (e.g. $e^+e^- \rightarrow (e)\tilde{e}\tilde{\gamma}$)

(d): new particle in the propagator (e.g. $e^+e^- \rightarrow \gamma\gamma$ via e^+ exchange).

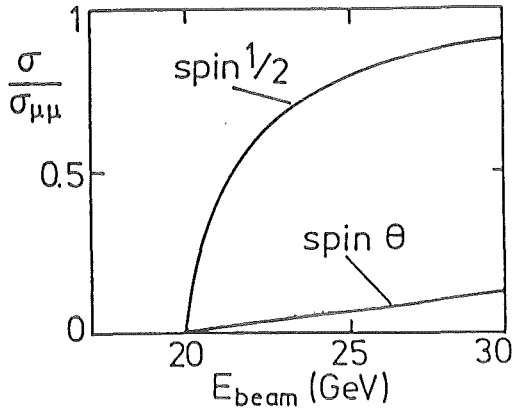


Figure 2: Threshold behavior for pair production of a $m = 20$ GeV, $|Q| = 1$ particle with spin 0 and spin 1/2.

by a β^3 threshold factor and by a factor 1/4 due to spin statistics. Neutral particles can be pair produced by annihilation into a (at present energies virtual) Z^0 . For instance, at present PETRA energy ($\sqrt{s} = 44$ GeV) the neutrino pair production cross section is:

$$\sigma(e^+e^- \rightarrow Z^0 \rightarrow \nu_\mu \bar{\nu}_\mu) = 1.1 pb$$

Correspondingly, the total cross section for Z^0 production at PETRA is

$$\sigma(e^+e^- \rightarrow Z^0 \rightarrow anything) = \frac{\sigma(e^+e^- \rightarrow Z^0 \rightarrow \nu_\mu \bar{\nu}_\mu)}{BR(Z^0 \rightarrow \nu \bar{\nu})} = 19 pb.$$

This means that ~ 900 Z^0 's have been produced at each of the four PETRA interaction regions. Seen this way, at present PETRA (and PEP) are the largest Z^0 factories available! This large production rate opens up the possibility to search for unusual Z^0 decays at present energy e^+e^- colliders. (c.f. searches for monojets from Z^0 decays at PETRA and PEP [1] which will not be discussed here.)

Obviously, pair production of new particles is limited to masses below the beam energy. Higher masses can be probed in the associated production of a charged particle together with a (possibly light) neutral one in $e\gamma$ collisions (Fig. 1c). This process is sensitive to masses up to $\sqrt{s} - m_{X^0}$.

Particles with masses above the c.m. energy can still be detected as virtual particles in the propagator (Fig. 1d).

Although limited in the available c.m. energy, as compared to hadron colliders, e^+e^- machines offer a very clean laboratory where potential new processes would stick out clearly over a well understood background.

Each of the four PETRA experiments now has collected a data sample of $\sim 50 pb^{-1}$ at c.m. energies around 44 GeV with a peak energy of 46.78 GeV. During the last shutdown in winter 85/86 RF cavities were removed and PETRA is running now at $\sqrt{s} = 35$ GeV. The reason for running at this reduced energy is a threefold increase in luminosity compared to the high energy running.

In this review I will concentrate on the following topics on most of which new results were obtained recently:

- Search for Heavy Leptons
 1. charged
 2. neutral
- Supersymmetry
 1. searches for $\tilde{\epsilon}$ and $\tilde{\gamma}$ (in particular search for single photons)
 2. searches for gauginos (\tilde{z} and \tilde{w}) and higgsinos
- Compositeness
 1. limits on the preon mass scale
 2. search for excited leptons (e^* , μ^* , τ^*)
 3. search for leptoquarks

For a summary of searches not covered here I refer to previous reviews [1].

2 Heavy Leptons

The repetitive nature of the three known fermion generations suggests a search for new leptons of a possible fourth generation.

2.1 Charged Heavy Lepton

A new charged lepton would be pair produced via one photon annihilation with a cross section (neglecting Z^0 effects)

$$\sigma(e^+e^- \rightarrow L^+L^-) = \frac{\beta(3 - \beta^2)}{2} \sigma_{\mu\mu}$$

where $\sigma_{\mu\mu}$ is the μ pair cross section.

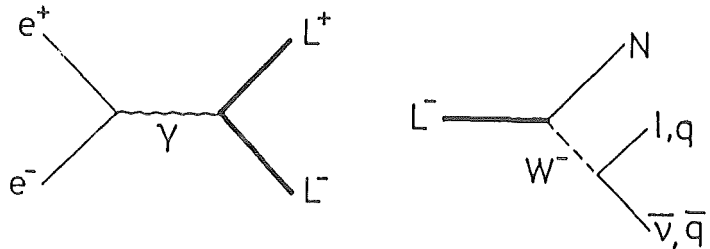


Figure 3: Pair production and decay of a sequential heavy lepton.

It is expected to decay via W exchange into a lighter lepton and neutrinos or into hadrons and neutrino with a leptonic branching fraction of $\sim 3 \cdot 11\%$. A general signature is missing energy and momentum carried away by neutrinos (Fig. 4).

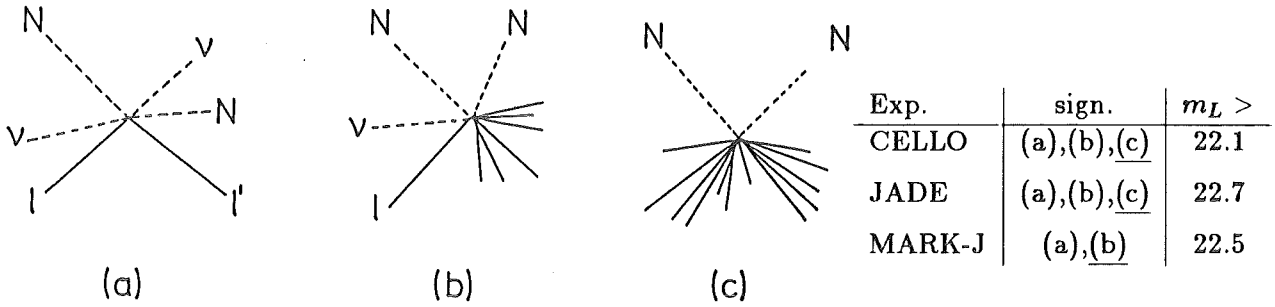


Figure 4: Signatures of heavy lepton pair production and decay. The table summarizes recent PETRA limits. The signature from which the actual limit was derived is underlined.

CELLO [2], JADE [3], and MARK-J [4] searched for these signatures in their high energy data obtaining lower mass limits of 22.1, 22.7, and 22.5 GeV respectively. These limits assume a vanishing mass for the fourth generation neutrino although they are quite insensitive to m_N and hold up to $m_N \lesssim 3/4 m_L$.

2.2 Neutral Heavy Lepton

One should not be discouraged by the fact that a charged fourth generation lepton must be too heavy to be produced at PETRA. When looking at the lepton mass spectrum (Fig. 5) one observes that there is plenty of room for massive neutrinos, in particular since there may be indications of a finite electron neutrino mass [5]. A multi-GeV fourth generation neutrino together with a charged lepton above 22 GeV would fit nicely into this mass pattern. A heavy neutrino can be pair produced in e^+e^- annihilation via Z^0 exchange with a cross section of

$$\sigma(e^+e^- \rightarrow N\bar{N}) = \frac{\beta(3+\beta^2)}{4} \sigma_{\nu_\mu\nu_\mu} \quad \sigma_{\nu_\mu\nu_\mu} = 1.1 \text{pb at } \sqrt{s} = 44 \text{GeV}$$

If the neutrinos had a finite mass, mixing between the lepton generations would occur and the new heavy neutrino would decay via W exchange into leptons and a neutrino (BR $\sim 3 \cdot 11\%$ if $m_N > m_\tau$) or into lepton and quarks (BR $\sim 67\%$). The lifetime depends on the neutrino mass and on the mixing matrix element U_{Ni} :

$$\tau_N = \frac{m_\mu^5}{m_N^5} \tau_\mu \frac{BR(N \rightarrow l\nu)}{\sum_l |U_{Ni}|^2}$$

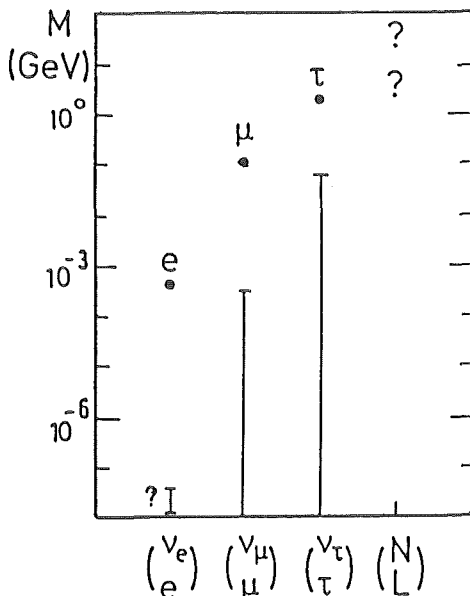


Figure 5: Mass pattern of the first three lepton generations. Also indicated are the present limits on neutrino masses [5]. There are indications of a finite ν_e mass in the range from 17 - 40 eV although another group quotes a limit of < 20 eV.

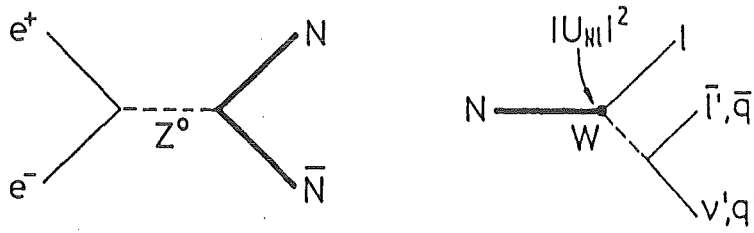


Figure 6: Pair production and charged current decay of a heavy neutrino.

CELLO [6] has searched for heavy neutrino pair production considering the following decay signatures:

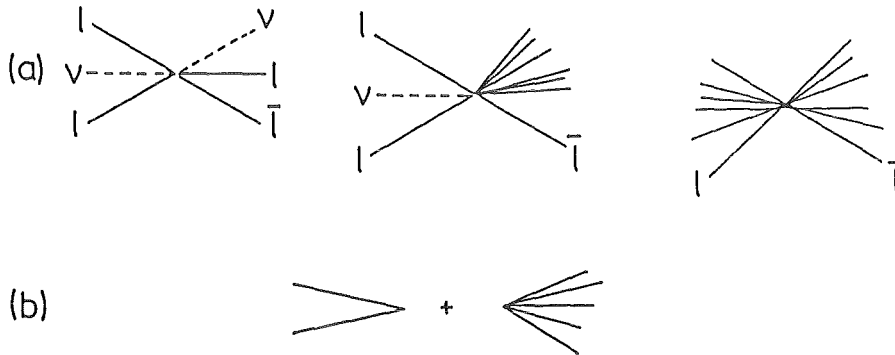


Figure 7: Signatures of heavy neutrino pair production investigated by CELLO

(a): mixing matrix element sufficiently large to give a short decay length less than ~ 1 cm. In all three cases there are at least two leptons.

(b): flight path sufficiently long to give rise to two separated secondary vertices inside the tracking chamber.

2.2.1 short lived heavy neutrino

To study this case use was made of the (at least) two leptons in the final state. The basic selection requirements were

- 2 leptons (e or μ) of the same flavour and opposite charge, one of them isolated by at least 18°
- at least two more additional tracks

For events with exactly four tracks some missing energy and momentum was required to suppress α^4 QED background from $e^+e^- \rightarrow ee ll$.

Two candidate events (one $e^+e^- X$ and one $\mu^+\mu^- X$) were observed compatible with the expected background from α^4 QED processes. Supposing for the moment that U_{Ne} or $U_{N\mu}$ is large enough such that the decay occurs close to the interaction region, the following neutrino mass range can be excluded at 95 % C.L.:

$$3.1 \text{ GeV} < m_N < 18.0 \text{ GeV} \quad \text{if N-e coupling dominant}$$

$$3.2 \text{ GeV} < m_N < 17.4 \text{ GeV} \quad \text{if N-}\mu \text{ coupling dominant}$$

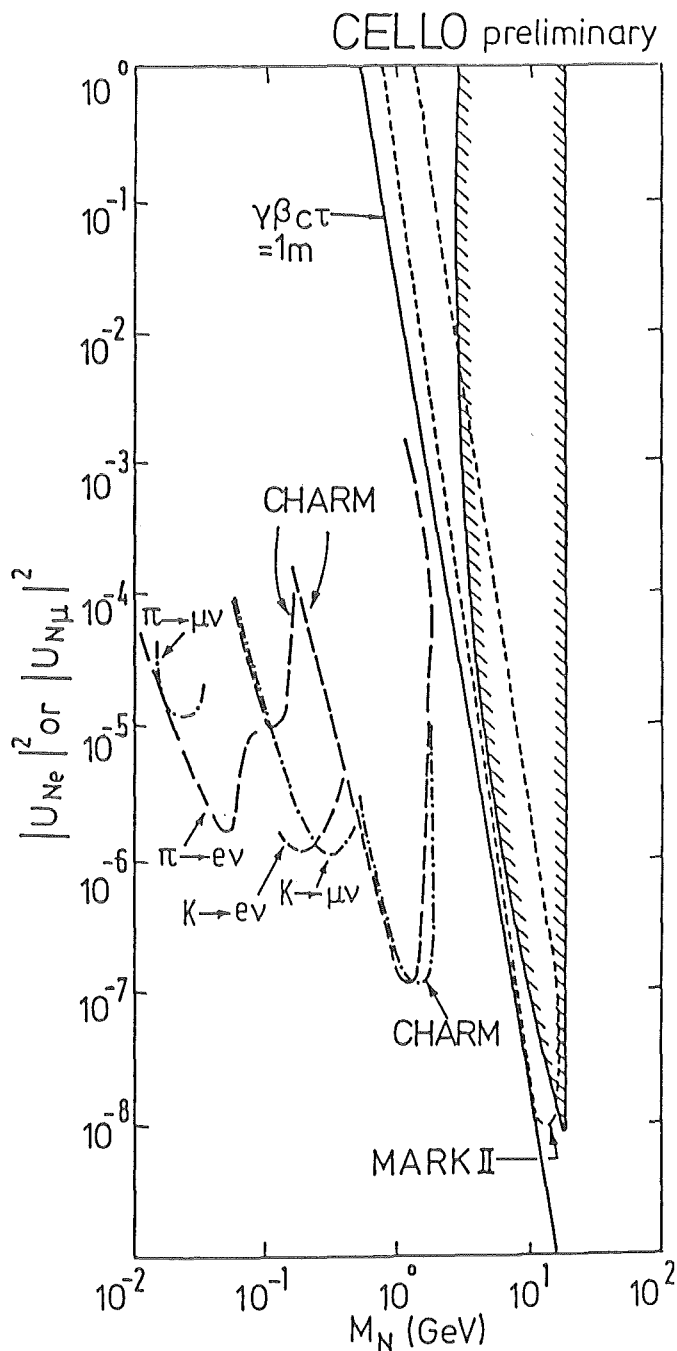


Figure 8: Limits on $|U_{Ne}|^2$ or $|U_{N\mu}|^2$ as function of the heavy neutrino mass. Also indicated are previous limits on $|U_{Ne}|^2$ (dashed lines) and $|U_{N\mu}|^2$ (dash-dotted lines) from π and K decays and from the CHARM experiment. For comparison, also a recent limit from a secondary vertex search at MARK II is shown [7]. The diagonal line corresponds to a neutrino flight path $\gamma\beta c\tau = 1m$ for $e^+e^- \rightarrow N\bar{N}$ at $\sqrt{s} = 44$ GeV.

2.2.2 long lived heavy neutrino

To extend the sensitivity to smaller mixings between the lepton generations and thus larger N lifetimes, a search for secondary vertices was made. The essential cuts were

- at least four charged particle tracks
- an average impact parameter d of the tracks $\geq 1\text{cm}$
- at least half of the tracks should have $d \geq 1\text{cm}$

After a visual scan no candidate event with two separate vertices is observed.

Fig. 8 shows the excluded heavy neutrino mass region as a function of the mixing with the first or second generation. This analysis improves the existing limits in the high mass region. Note, however, that the limit in this form holds only if either $|U_{Ne}|^2$ or $|U_{N\mu}|^2 \gg |U_{N\tau}|^2$.

standard particle	$ \Delta j = 1/2$	SUSY partner
$j = 1/2$ $q_L, q_R \quad q = u, d, s, \dots$ $l_L, l_R \quad l = e, \mu, \tau$ ν_L		$j = 0$ $\tilde{q}_L, \tilde{q}_R \quad q = u, d, s, \dots$ $\tilde{l}_L, \tilde{l}_R \quad l = e, \mu, \tau$ $\tilde{\nu}_L$
$j = 1$ γ Z^0, W		$j = 1/2$ \tilde{g} <div style="display: flex; justify-content: space-around; border: 1px dashed black; padding: 5px;"> <div style="border-right: 1px dashed black; padding: 2px 5px;"> $\tilde{\gamma} \quad \tilde{z}$ </div> <div style="padding: 2px 5px;"> \tilde{w}^\pm </div> </div> <div style="display: flex; justify-content: space-around; border: 1px dashed black; padding: 2px 5px;"> <div style="border-right: 1px dashed black; padding: 2px 5px;"> Neutralinos $\tilde{h}_1^0 \quad \tilde{h}_2^0$ </div> <div style="padding: 2px 5px;"> Charginos \tilde{h}^\pm </div> </div>
$j = 0$ $H_1^\pm \quad H_2^0$ $H_1^0 \quad H_2^\pm$		\tilde{G} Goldstino
		$j = 3/2$ \tilde{G} Gravitino

Table 1: The Standard Model particles spectrum together with the minimal supersymmetric extension.

3 Supersymmetry

The main feature of supersymmetric models [8] is the prediction of a partner for each known particle with the same couplings and quantum numbers except spin which differs by $|\Delta j| = 1/2$. In this case many divergencies in Feynman graphs are cancelled, since the fermions and bosons contribute equally with opposite signs, provided the supersymmetric particles are not too heavy. The absence of mass degenerate supersymmetric partners of the known particles shows that supersymmetry must be broken. The details of this symmetry breaking are unknown. Therefore there are no firm predictions for the masses of the supersymmetric particles.

Table 1 summarizes the minimal SUSY extension of the Standard Model. Note that two Higgs doublets are needed to preserve the one to one correspondence between Higgs and higgsino states. In general, the SUSY partners of the gauge bosons and the Higgs particles are expected to mix forming so-called neutralino and chargino mass eigenstates.

SUSY particles carry a (in most models) conserved quantum number R-parity. For this reason, they can be produced only in associated production. Of particular phenomenological importance is the lightest SUSY particle (LSP) since all SUSY particles eventually will decay into it. It is favoured to be uncolored and neutral. Moreover it is stable (R-parity conservation) and only weakly interacting, i.e. ν -like. Therefore a general signature for supersymmetric processes is missing energy and momentum carried away by the LSP. LSP candidates are [9] the photino, the neutral higgsino the scalar neutrino, or a spin 1/2 Goldstino \tilde{G} appearing in globally supersymmetric models [10].

3.1 Unstable Photino

If a light Goldstino is the LSP the photino is expected to decay into a photon and a Goldstino (see Fig. 9b) with a lifetime $\tau = 8\pi d^2 / m_\gamma^5$ (see Ref. [11]) where d characterizes the scale of supersymmetry breaking. In locally supersymmetric models, however, the Goldstino is absorbed into a massive spin 3/2 gravitino.

Another LSP candidate is the neutral higgsino. In this case the photino would decay into a photon and a higgsino (see Fig 9c). For a wide range of parameters ($m_\gamma, m_{\tilde{h}}, m_t, m_{\tilde{\nu}}, \tilde{\gamma} - \tilde{h}$ mixing) the photino lifetime is sufficiently short such that the decay occurs inside a detector [12]. This scenario

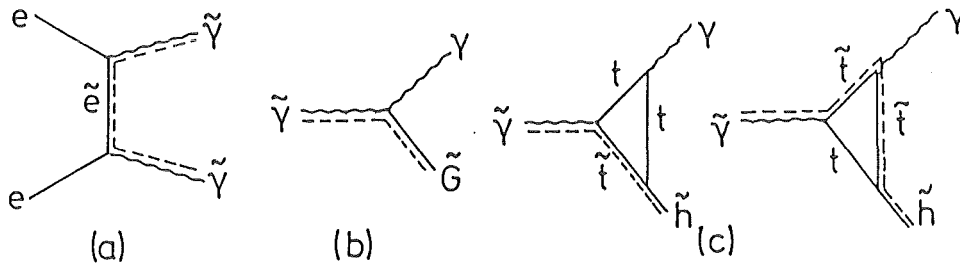


Figure 9: Diagrams for photino pair production (a) and decay into photon and Goldstino (b) or photon and higgsino (c).

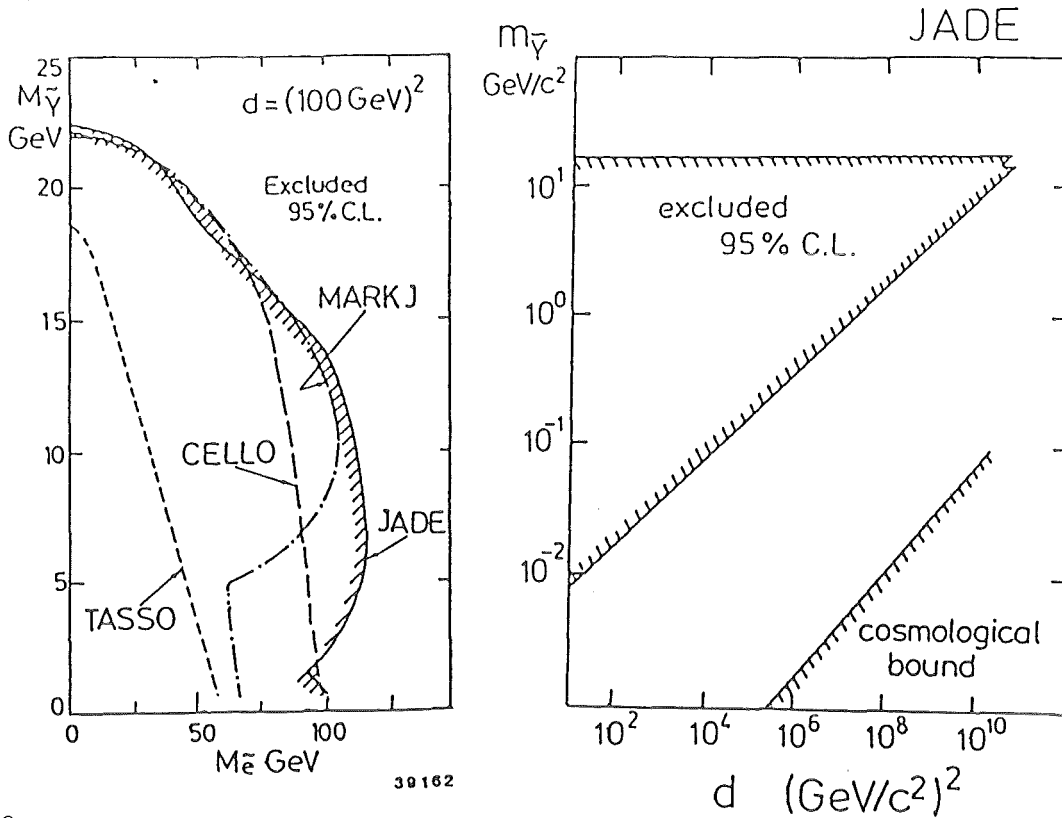


Figure 10:

- (a): Excluded domain in photino and scalar electron mass for unstable photinos decaying inside the detector.
- (b): Excluded $\tilde{\gamma}$ mass as function of the SUSY breaking scale d (assuming $m_{\tilde{\gamma}} = 40$ GeV).

was discussed by G.L. Kane [13] as a possibility to weaken the missing p_t signature of photinos, thus making more room for SUSY reactions in the $p\bar{p}$ collider data.

Photinos can be pair produced in e^+e^- interactions by t-channel exchange of a scalar electron (see Fig. 9a.). The subsequent decay into photon and one of the LSP's discussed above produces, in case of a heavy photino, an acoplanar pair of photons with missing energy and momentum carried away by the unobserved LSP's, whereas for a light photino its decay photons are boosted into the original photino direction giving rise to a pair of collinear photons with missing energy. All four PETRA experiments [14,15,16,17] looked for these signatures and did not observe any candidates.

Fig 10a shows the status of the relevant searches. The indicated region in photino and scalar electron mass is excluded if the photino decays inside the detector in a photon and a light penetrating particle, independent of any specific model. For this reason further searches discussed below assume

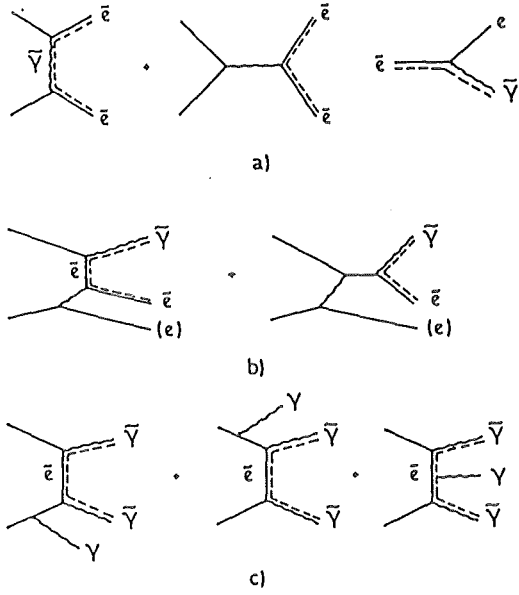


Figure 11: \tilde{e} and $\tilde{\gamma}$ production processes in e^+e^- annihilation

- (a): \tilde{e} pair production
- (b): single \tilde{e} production
- (c): radiative $\tilde{\gamma}$ pair production

an invisible photino (either stable or long lived or decaying invisibly, e.g. into $\tilde{\nu}\nu$).

Fig. 10b indicates the excluded domain in photino mass and SUSY breaking scale d in the framework of the light Goldstino model discussed above.

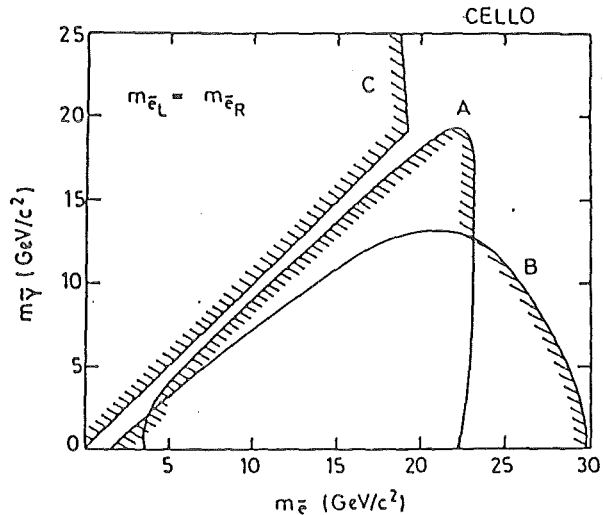
3.2 Combined Searches for \tilde{e} and $\tilde{\gamma}$, invisible $\tilde{\gamma}$

Searches for scalar electrons and photinos have been carried out by looking for the processes shown in Fig. 11.

Pair production of \tilde{e} 's followed by the decay $\tilde{e} \rightarrow e\tilde{\gamma}$ results in an acoplanar pair of electrons and missing energy and momentum in the unobserved photinos. Obviously, this process is limited to $m_{\tilde{e}} < E_{beam}$.

Higher \tilde{e} masses up to $\sqrt{s} - m_{\tilde{\gamma}}$ can be reached in the production of a single \tilde{e} and a $\tilde{\gamma}$ in the collision of a beam electron with a radiated quasi real photon (Fig. 11b.). The signature for

Figure 12: \tilde{e} and $\tilde{\gamma}$ masses excluded from pair production (contour A), and single production (contour B) of scalar electrons. Contour C indicates a limit on stable scalar electrons.



single γ trigger threshold ($\epsilon = 50\%$)	2.0 GeV $\hat{=}$ $x_\gamma \simeq .1$
search region	$ \cos\Theta_\gamma < .83$
minimum veto angle Θ_{min}	50mrad $\hat{=}$ $x_{t\gamma} = .05$
time resolution on showers	$\Delta t = 45(25)ns$ for $E_\gamma = 2(> 4)GeV$
shower angular resolution	3.5° in two projections
data sample	37 pb ⁻¹ at $\sqrt{\langle s \rangle} = 42.6$ GeV

Table 2: Summary of the CELLO detector parameters relevant to the single photon search.

this reaction is a single hard electron from the \tilde{e} decay and nothing else in the detector (the second electron escapes unobserved along the beam pipe).

\tilde{e} pair production was studied by all four PETRA experiments [13,18,16,19] while single \tilde{e} production was investigated by CELLO [13] and JADE [18]. The CELLO limits on \tilde{e} and $\tilde{\gamma}$ mass are indicated in Fig. 12.

3.3 Search for Single Photons (CELLO)

CELLO [20] studied a third possibility to search for scalar electrons and photinos, namely to tag (invisible) $\tilde{\gamma}$ pair production by a photon radiated in the initial state (Fig. 11c) very similar to the ν -counting reaction $e^+e^- \rightarrow \gamma\nu\bar{\nu}$. The signature is a single photon in the detector and nothing else. The single photon spectrum is of the Bremsstrahlung type peaked at low energies and small angles with respect to the electron beam. This requires a low trigger threshold for single photons and a large acceptance for the trigger photon.

In order to be able to reject QED background from radiative Bhabha scattering and photon pair production hermetic calorimetry down to small angles is essential (see Fig. 13).

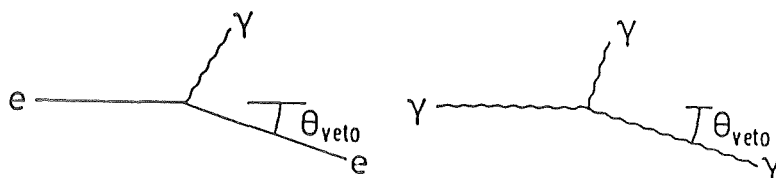


Figure 13: QED background processes in the single photon search. This background can be kinematically excluded by a hermetic e.m. calorimetry if $x_{t\gamma} = E_{t\gamma}/E_{beam} > 2\Theta_{min}$. For practical purposes $x_{t\gamma} \gtrsim \Theta_{min}$ is sufficient since the dominant background contribution is the virtual Compton configuration of Bhabha scattering where one electron is scattered under $\sim 0^\circ$.

Another important background are cosmic showers in the calorimeter. They can be suppressed by

1. timing cuts on the calorimeter energy sum signals,
2. requiring that the shower points back to the interaction region,
3. cuts on the lateral and longitudinal shower development and
4. on the hit pattern in the central drift chamber.

Fig. 14 shows a single photon event in the CELLO detector and Table 2 summarizes the relevant detector parameters.

The ultimate background for this reaction are single photons from radiative neutrino pair production.

After an automatic selection requiring a single photon ($x_t = E_t/E_{beam} > .05$) in the barrel calorime-

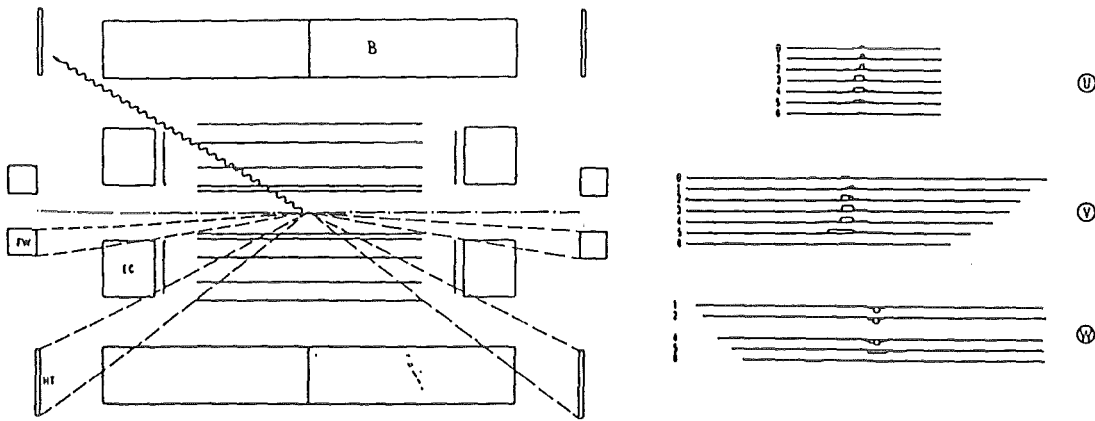


Figure 14: Example of an event with a single photon in the barrel calorimeter vetoed in the hole tagger.

(a): The various components of calorimetric coverage are indicated: barrel (B) and end cap (EC) lead-liquid argon calorimeter, hole tagger (HT, a simple lead scintillator to veto photons between barrel and end cap calorimeter) and forward lead glass array (FW). The wiggled line indicates the direction of the additional photon detected in the hole tagger.

(b): Data of the calorimeter module containing the shower. The lead strips of the seven layers in the U direction run parallel to the beam, those of the 7 layers in V direction transverse to it, and those of the 5 layers in W direction at 45° with respect to U and V. The magnification varies with depth such that a shower pointing to the interaction vertex always appears perpendicular to the layers.

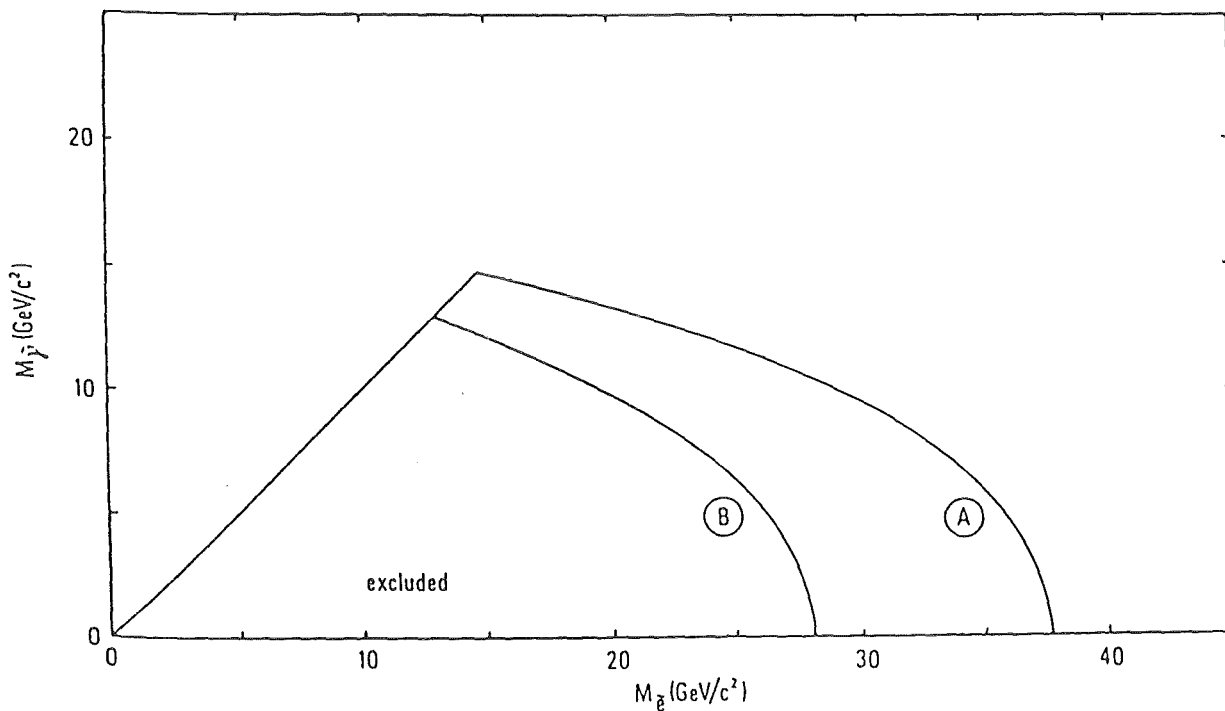


Figure 15: 90% C.L. limits on \tilde{e} and $\tilde{\tau}$ mass obtained by the search for single photons assuming mass degenerate partners of the left- and right-handed electron (A) or $m_{\tilde{\nu}_{eL}} \gg m_{\tilde{\nu}_{eR}}$ (B).

ter and no other signals in the detector and applying cosmic rejection cuts 30 events remained. They could be unambiguously rejected by a visual scan as beam gas or beam wall interactions with unreconstructed tracks or as cosmic showers, thus leaving no candidate event. The efficiency of the trigger and the selection procedure was monitored by control samples of

1. single electron events from radiative Bhabha scattering triggered by a hit in the end cap or forward calorimeter,
2. photons from $ee\gamma$ final states, and
3. 'empty' events taken at random beam crossings.

For the analyzed data sample .68 events are expected from radiative ν pair production giving a 51 % probability to observe no event. The 90 % C.L. upper limit on the number of light neutrino species obtained from this analysis is 14.9. Combining this result with the most recent ones obtained by ASP [21] and MAC [22] in a similar analysis, one obtains a 90% (95%) C.L. limit of 8(10) on the total number of light neutrinos.

Interpreting this result in terms of photino pair production, the $\tilde{\epsilon}$ and $\tilde{\gamma}$ mass region indicated in Fig. 15 can be excluded.

3.4 Gauginos

The weak vector bosons W^\pm and Z^0 are too heavy to be produced at present energy e^+e^- colliders. On the other hand, many models predict their supersymmetric partners, the wino \tilde{w} and zino \tilde{z} , to be lighter. First we will assume the \tilde{z} and \tilde{w} to be unmixed and postpone the discussion of gaugino higgsino mixing.

3.4.1 Zinos

In e^+e^- interactions zinos can be produced together with a $\tilde{\gamma}$ via $\tilde{\epsilon}$ exchange (see Fig. 16a). The experimental signature for this reaction of course depends on the decay modes of the zino. Depending on the SUSY mass spectrum, various scenarios are possible:

heavy gluino ($m_{\tilde{g}} > m_{\tilde{z}}$), heavy sneutrino ($m_{\tilde{\nu}} > m_{\tilde{z}}$):

In this case the zino decays via scalar exchange into an fermion anti-fermion pair and a photino (diagram b,c in Fig. 16). In case of equal scalar quark and lepton masses one expects a leptonic branching fraction of 13 % per lepton generation. The signature is an acoplanar lepton resp. jet pair or, for smaller zino masses, a single jet with an empty opposite hemisphere.

light gluino ($m_{\tilde{g}} < m_{\tilde{z}}$):

In this case the dominant zino decay would be hadronically into $q\bar{q}\tilde{g}$ followed by $\tilde{g} \rightarrow q\bar{q}\tilde{\gamma}$ (diagrams d,m in Fig. 16), due to the stronger hadronic $\tilde{q}q\tilde{g}$ coupling. Also here one expects acoplanar jets resp. single jets.

light sneutrino ($m_{\tilde{\nu}} < m_{\tilde{z}}$):

Perhaps the scalar neutrino is the lightest SUSY particle [23]. Then the zino would decay exclusively into an invisible $\tilde{\nu}\nu$ final state (Fig. 16e) and the only possibility to put limits on its mass would be initial state radiation tagging similar to $e^+e^- \rightarrow \gamma\tilde{\gamma}\tilde{\gamma}$ and $e^+e^- \rightarrow \gamma\nu\nu$ discussed above.

MARK-J has searched for leptonic zino decays [24], while CELLO [14] and JADE [25] considered both hadronic and leptonic final states. Figs. 17a and b show excluded zino masses for different decay scenarios.

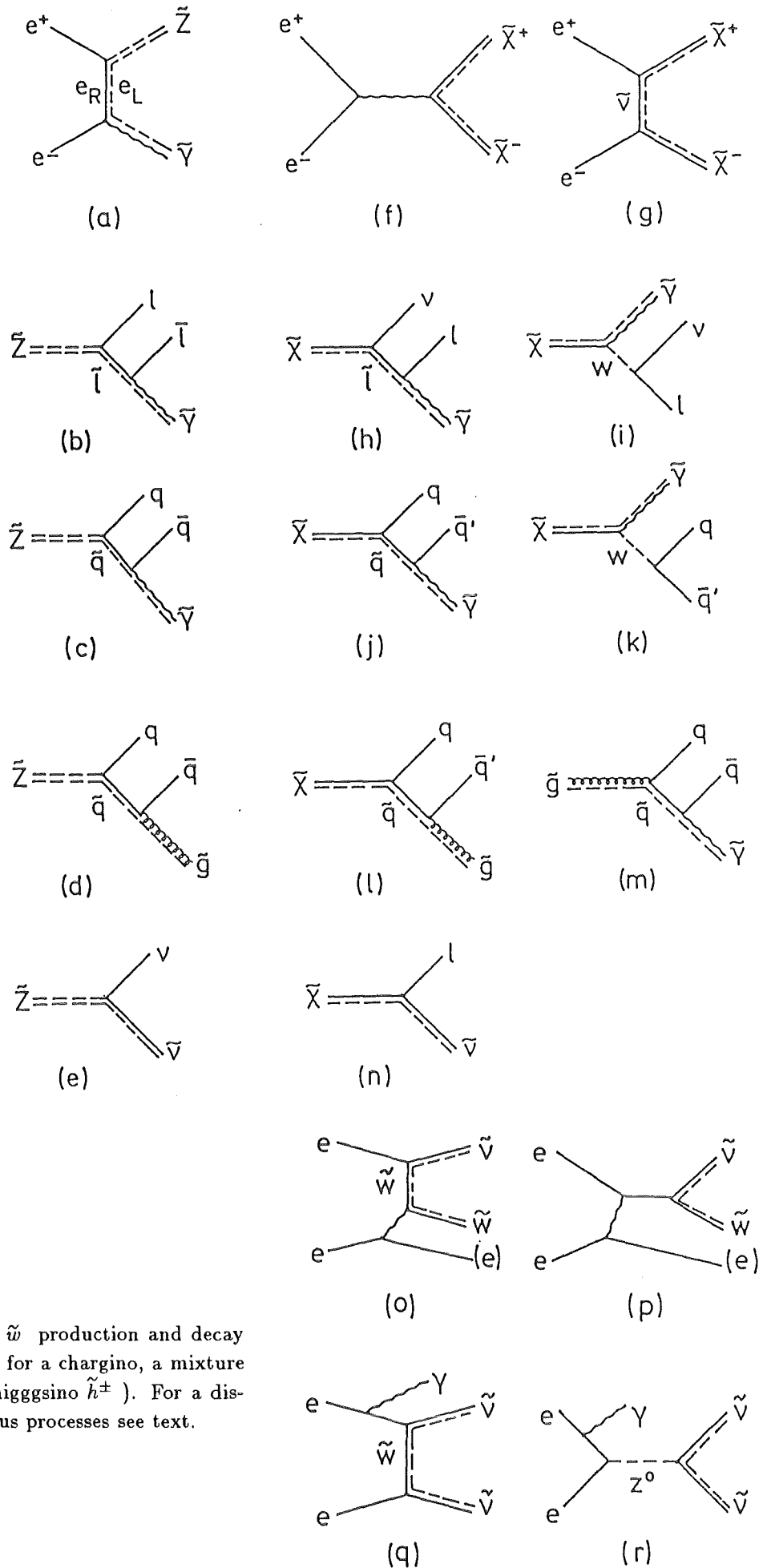


Figure 16: \tilde{z} and \tilde{w} production and decay processes ($\tilde{\chi}$ stands for a chargino, a mixture of \tilde{w} and charged higgsino \tilde{h}^\pm). For a discussion of the various processes see text.

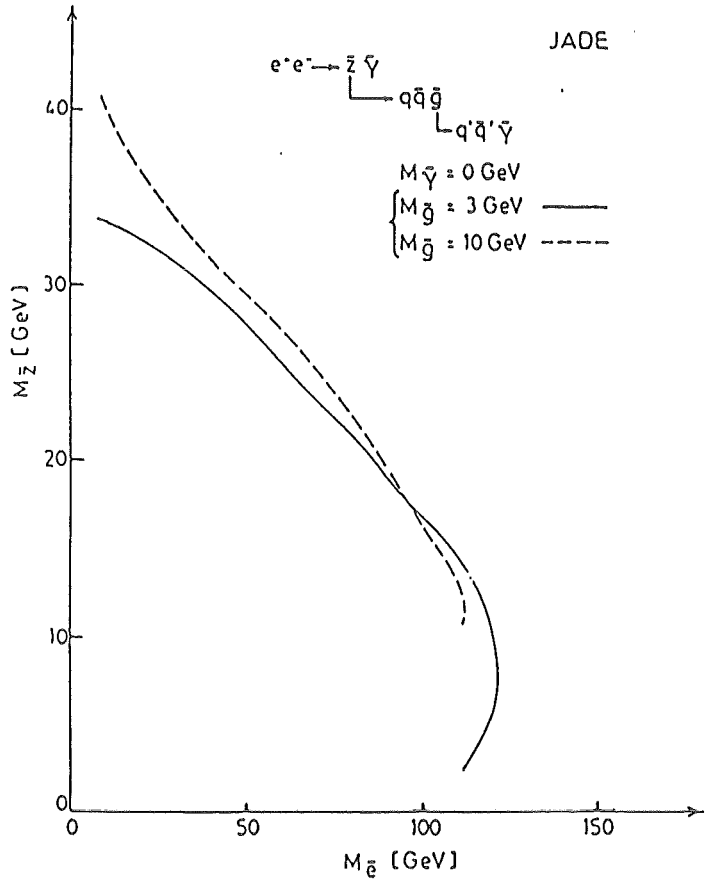
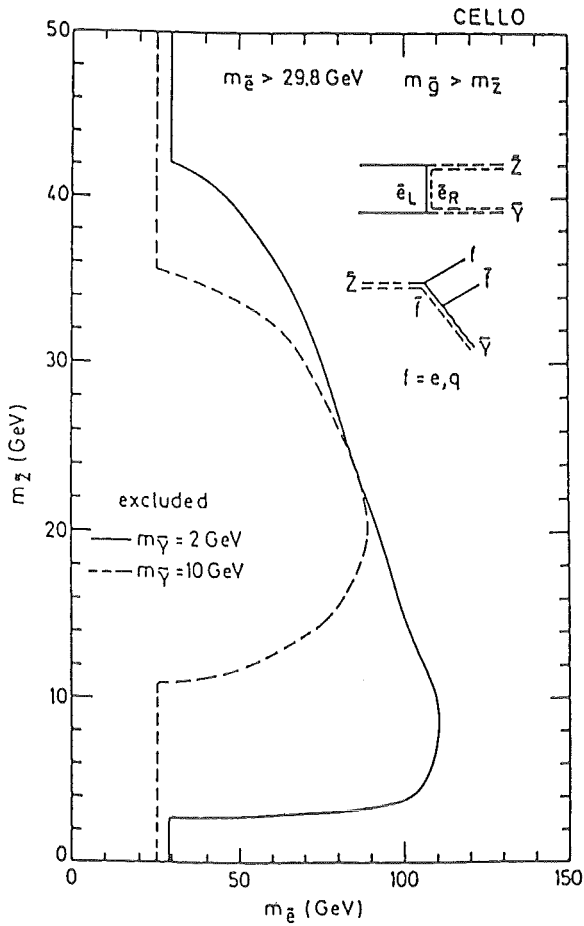


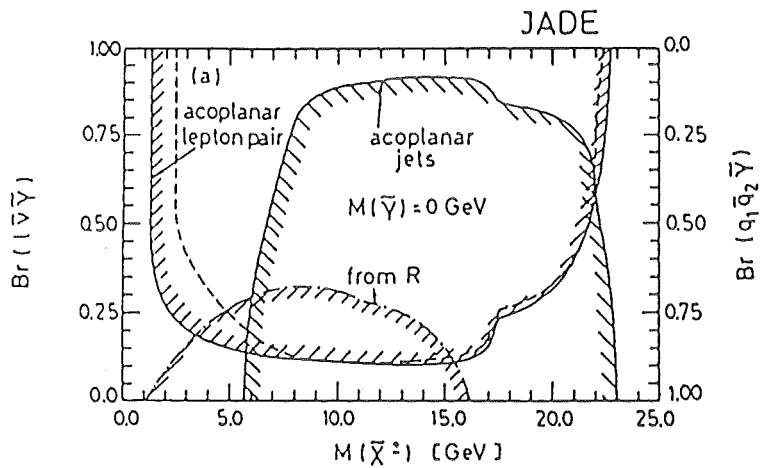
Figure 17: Limits on \tilde{z} production assuming $m_{\tilde{\nu}} > m_{\tilde{z}}$.

- (a): $m_{\tilde{g}} > m_{\tilde{z}}$, combined limit including searches for acoplanar leptons, acoplanar jets, and single jets.
- (b): $m_{\tilde{g}} < m_{\tilde{z}}$, assuming the zino to decay 100 % into $q\tilde{q}$.

Figure 18: Limits on \tilde{w} masses

(a):

$m_{\tilde{g}}, m_{\tilde{\nu}} > m_{\tilde{w}}$: excluded mass as a function of the wino leptonic branching ratio.



(b):

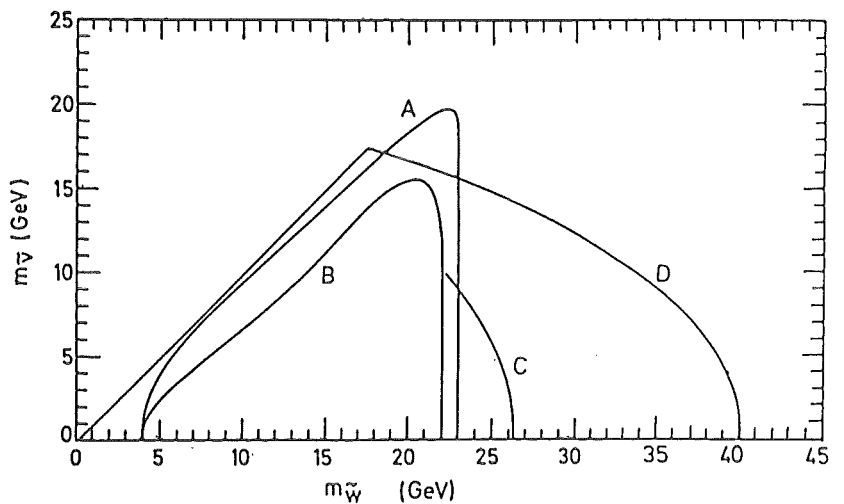
$m_{\tilde{\nu}} < m_{\tilde{w}}$: excluded \tilde{w} and $\tilde{\nu}$ masses

A $e^+e^- \rightarrow \tilde{w}^+\tilde{w}^-$ (equal decay widths into $e\tilde{\nu}, \mu\tilde{\nu}, \tau\tilde{\nu}$)

B $e^+e^- \rightarrow \tilde{h}^+\tilde{h}^-$ (100% branching ratio into $\tau\tilde{\nu}$)

C $e^+e^- \rightarrow (e)\tilde{w}\tilde{\nu}$

D $e^+e^- \rightarrow \gamma\tilde{\nu}\tilde{\nu}$



3.4.2 Winos

Winos can be pair produced via one photon annihilation and via t-channel sneutrino exchange. Similar to the zino case various decay scenarios are possible:

heavy gluino ($m_{\tilde{g}} > m_{\tilde{w}}$), heavy sneutrino ($m_{\tilde{\nu}} > m_{\tilde{w}}$):

The wino decays into $l\nu\tilde{\gamma}$ or $q\bar{q}'\tilde{\gamma}$ via W or via scalar exchange (Fig. 16 h-k) with a leptonic branching fraction of O(10%) per lepton generation. One expects acoplanar lepton and jet pairs.

light gluino ($m_{\tilde{g}} < m_{\tilde{w}}$):

The wino decays dominantly hadronically into $q\bar{q}'\tilde{g}$, followed by $\tilde{g} \rightarrow q\bar{q}\tilde{\gamma}$ (Fig. 16 l,m). Winos are pair produced, so that one has 8 quarks in the final state resulting in spherical events with relatively small missing p_t .

light sneutrino ($m_{\tilde{\nu}} < m_{\tilde{w}}$):

If the scalar neutrino is light the winos decays exclusively into $l\tilde{\nu}$ final states (Fig. 16n) with the sneutrino escaping unseen, resulting in a final state of two acoplanar leptons.

MARK-J[24] has looked for acoplanar leptons, while JADE[26] and CELLO[14] also searched for acoplanar jets (see Fig. 18). Moreover, CELLO and JADE looked for an excess of spherical events from $\tilde{w} \rightarrow q\bar{q}'\tilde{g}$ and exclude this decay mode for wino masses of up to 22.4 GeV. We can conclude that winos below 22 GeV are excluded for ALL potential wino decay modes.

If the scalar neutrino is light, wino masses above the beam energy can be probed by the single production of winos in $e\gamma$ collisions (see Fig. 16 o,p), the signature being a single lepton and an escaping sneutrino from the wino decay $\tilde{w} \rightarrow l\tilde{\nu}$. This process was studied by CELLO [14] and MARK-J [24]. Contour C in Fig. 18b indicates the CELLO limit. Pair production of scalar electron neutrinos via \tilde{w} exchange, tagged by an radiative photon (see Fig. 16 q,r), is sensitive to even higher \tilde{w} masses. \tilde{w} and $\tilde{\nu}$ masses excluded by the CELLO single photon search [20] are indicated by contour D in Fig. 18b.

3.4.3 Gaugino Higgsino Mixing

In general, photino, zino, and the neutral higgsinos are expected to mix forming so called neutralino mass eigenstates, while winos and charged higgsinos may mix forming charginos [27,28].

In $e^+e^- \rightarrow \tilde{\gamma}\tilde{z}$ a higgsino admixture in the zino would cause a lowered production cross section due to the small $\tilde{h}\tilde{z}e$ coupling while the zino decay properties would be essentially unaltered [27].

If the wino in $e^+e^- \rightarrow \tilde{w}^+\tilde{w}^-$ is replaced by a charged higgsino only the one photon annihilation amplitude contributes to production. The decay of a charged higgsino is expected to proceed via W exchange [28] giving a signature identical to wino pair production. In case the scalar neutrino is light the dominant decay will be $\tilde{h} \rightarrow \tau\tilde{\nu}$, giving rise to an acoplanar τ pair. CELLO and JADE also studied this signature (see Fig. 18, contour B) so that the limit $m > 22$ GeV also holds for a charged higgsino.

The cross section for single \tilde{w} production and $\tilde{\nu}$ pair production via \tilde{w} exchange, however, would be reduced by a higgsino admixture, so that these limits are valid only for a relatively pure wino.

4 Compositeness

Compositeness of all or part of the Standard Model particle zoo could show up experimentally either by deviations from Standard Model predictions in known processes or by direct production of new particles expected in composite models.

	η_{LL}	η_{RR}	$\eta_{RL} = \eta_{LR}$	CELLO	JADE	MARK-J	PLUTO	TASSO
Λ_{LL}^+	1	0	0	1.1	.8	.9	1.1	.7
Λ_{LL}^-	-1	0	0	1.2	1.5	1.0	.8	1.9
Λ_{RR}^+	0	1	0	1.1	.8	.9	1.1	.7
Λ_{RR}^-	0	-1	0	1.2	1.5	1.0	.8	1.9
Λ_{VV}^+	1	1	1	2.4	2.4	1.7	2.2	1.9
Λ_{VV}^-	-1	-1	-1	2.7	2.9	2.4	1.9	2.9
Λ_{AA}^+	1	1	-1	1.9	2.2	2.3	2.0	2.0
Λ_{AA}^-	-1	-1	1	2.5	2.7	.9	1.6	2.3

Table 3: 95% C.L. limits on the preon mass scale (in TeV) obtained from Bhabha scattering by CELLO [30], JADE [31], MARK-J [32], PLUTO [33], and TASSO [34].

4.1 Limits on the Preon Mass Scale

If the fermions were built from preons one, would expect residual contact interactions which would modify cross sections for Standard Model processes. In Bhabha scattering, for instance, an additional contact interaction amplitude besides γ and Z^0 exchange would show up (Fig. 19).

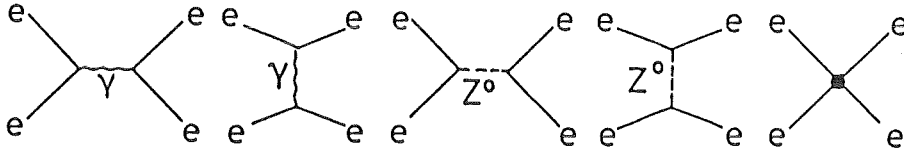


Figure 19: The lower order amplitude for $e^+e^- \rightarrow e^+e^-$ in the Standard Model and and the additional amplitude due to contact interactions expected in preon models.

A model independent parametrisation for this contact interaction was proposed by Eichten et al. [29]:

$$L_{contact} = \frac{g^2}{2\Lambda^2} \sum_{i,j=L,R} \eta_{ij} \cdot \bar{\psi}_i \gamma_\mu \psi_i \cdot \bar{\psi}_j \gamma^\mu \psi_j \quad (1)$$

were g is the preon coupling constant and Λ is the preon mass scale. Fig. 20 illustrates the expected deviation in the differential Bhabha scattering cross section for compositeness scales of order TeV.

Table 3 summarizes the PETRA limits on the preon mass scale from Bhabha scattering. The preon binding force is assumed to be strong ($g^2/4\pi = 1$) at present Q^2 .

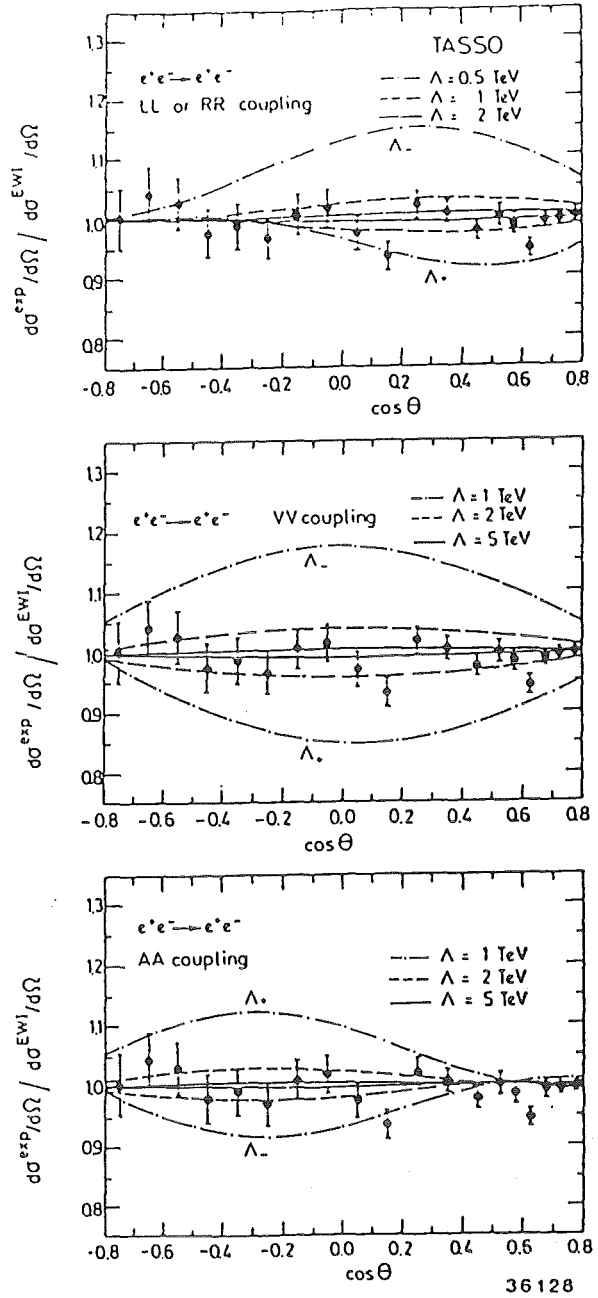


Figure 20: The differential cross section for $e^+e^- \rightarrow e^+e^-$ normalized to the Standard Model expectation together with the deviations expected for different preon mass scales and assumptions on the chiral structure of the contact interaction. The preon binding force is assumed to be strong ($g^2/4\pi = 1$).

4.2 Search for Excited Leptons

The most direct evidence for lepton compositeness would come from the observation of excited lepton states l^* decaying into the lepton ground state and a photon. This decay involves a γll^* coupling which can be described by the following Lagrangian

$$L_{int} = \lambda \frac{e}{2M^*} \bar{\psi}^* \sigma_{\mu\nu} \psi F^{\mu\nu} + \text{h. c.} \quad (2)$$

where M^* is the excited lepton mass and λ is a dimensionless parameter describing the strength of this coupling relative to the normal QED type coupling.

Excited leptons can be pair produced (Fig. 21 a,b) giving rise to a $ll\gamma\gamma$ final state with two equal mass $l\gamma$ mass combinations. Amplitude (a) is independent of the coupling strength λ . Possible form

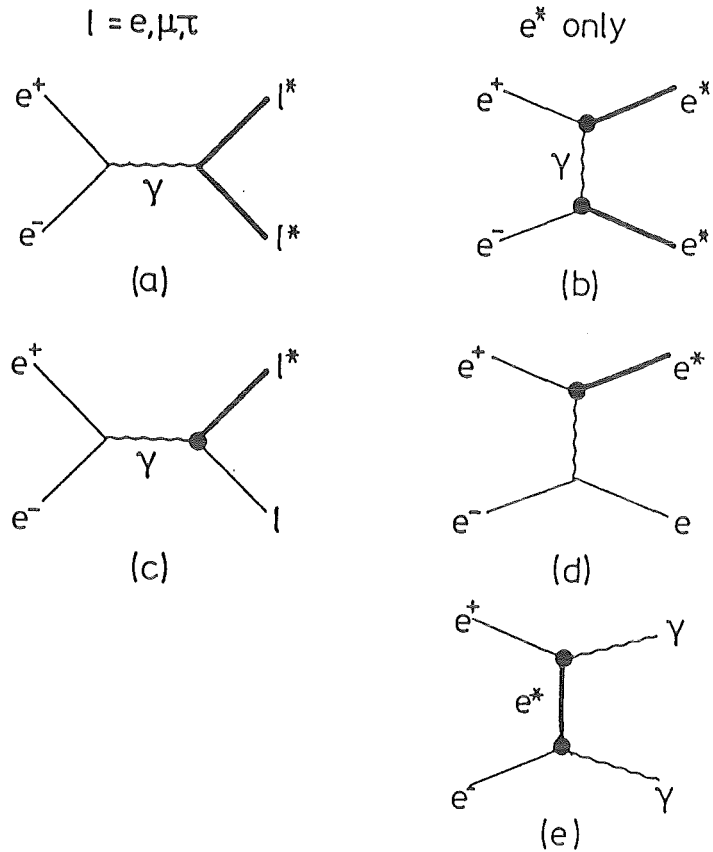


Figure 21: Excited lepton production mechanisms (a - d), pair production (a, b) and single production (c, d). Diagrams (b) and (d) are for excited electrons only. (e) shows photon pair production via e^* exchange. The full circles indicate a γll^* coupling proportional to the (unknown) coupling strength λ in equation 2.

factor effects can be safely neglected at present energies since the compositeness scale must be greater than a few TeV as discussed before. CELLO [35] (JADE) have searched for this signature in their high energy data and obtain 95% C.L. mass limits for the e^* , μ^* , and τ^* of 23.0 (23.1 [1]), 23.0, and 22.7 (22.5 [36]) GeV respectively, independent of λ .

l^* masses above the beam energy can be probed by single l^* production via diagrams (c, d) in Fig. 21, giving rise to $ll\gamma$ final states. Background from α^3 QED processes can be suppressed by looking for a peak in the $l\gamma$ invariant mass spectrum (Fig. 22). In case of single e^* production the 'virtual Compton' configuration of diagram (D) is dominant [37] for the mass region of interest ($m_{l^*} > E_{beam}$). Here one electron is scattered under a small angle and stays unobserved in the beam pipe giving rise to an $e\gamma$ final state from the e^* decay.

A virtual e^* in the propagator (Fig. 21e) modifies the $e^+e^- \rightarrow \gamma\gamma$ cross section even for e^* masses above the c.m. energy.

Fig. 23a shows limits from CELLO [35] and JADE [1] on λ as function of the the e^* mass from pair production (independent of λ), single production, and e^* propagator effects in $e^+e^- \rightarrow \gamma\gamma$. Fig. 23b indicates the corresponding limits for excited μ 's and τ 's.

4.3 Search for Leptoquarks

4.3.1 The CELLO dimuon event

As a motivation for the following discussions on leptoquarks I would like to remind the reader of a peculiar dimuon dijet event observed by the CELLO collaboration back in 1984 [38] at $\sqrt{s} = 43.45$ GeV. Fig. 24a shows the event in momentum space. Remarkable properties are

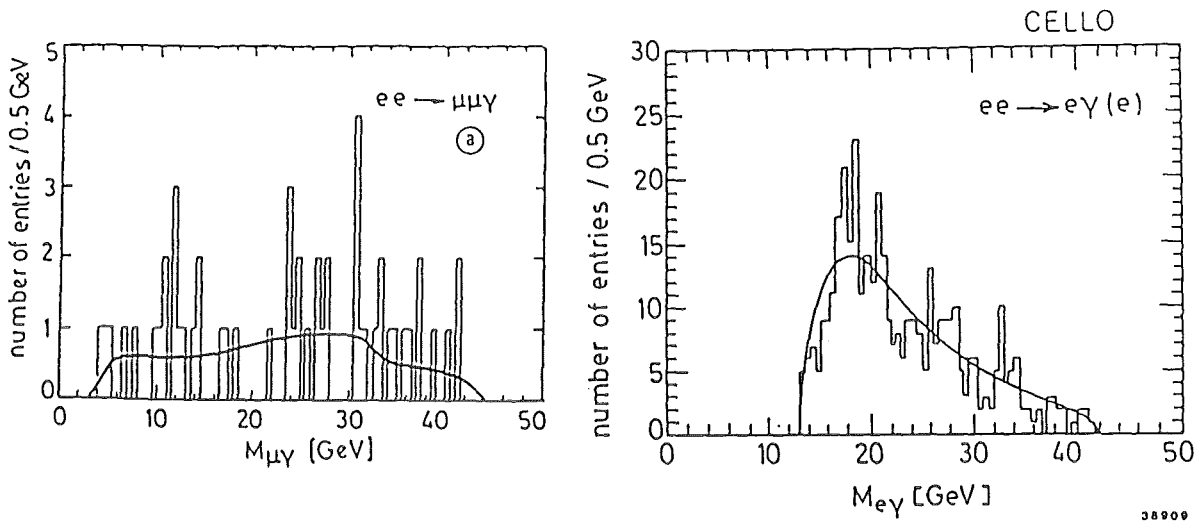


Figure 22: Invariant $l\gamma$ mass spectrum for $\mu\mu\gamma$ (a, 2 entries per event) and $(e)e\gamma$ (b, 1 entry per event) final states together with the expectation from α^3 QED. The $l\gamma$ mass resolution obtained by kinematic fitting is ~ 300 MeV in both cases. No significant peak is observed.

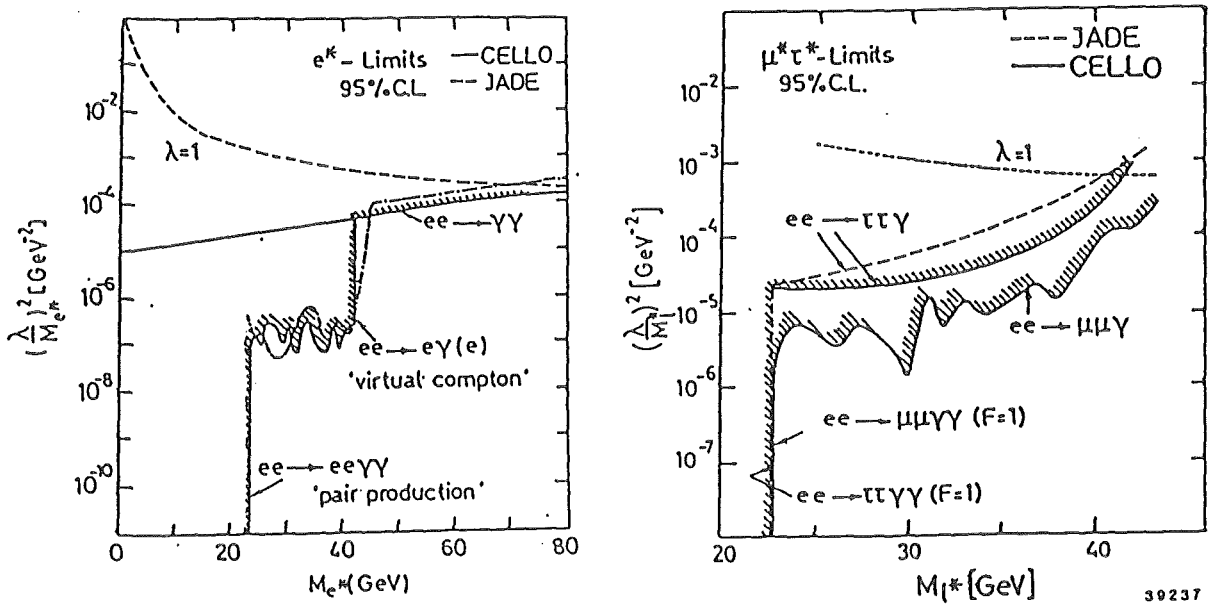


Figure 23: Limits on excited lepton couplings λ as function of the l^* mass for an excited electron (a) and for excited μ^* 's and τ^* 's (b). The wiggleness of the limit from single e^* and single μ^* production reflects statistical fluctuations in the $l\gamma$ invariant mass spectrum (see Fig. 22).

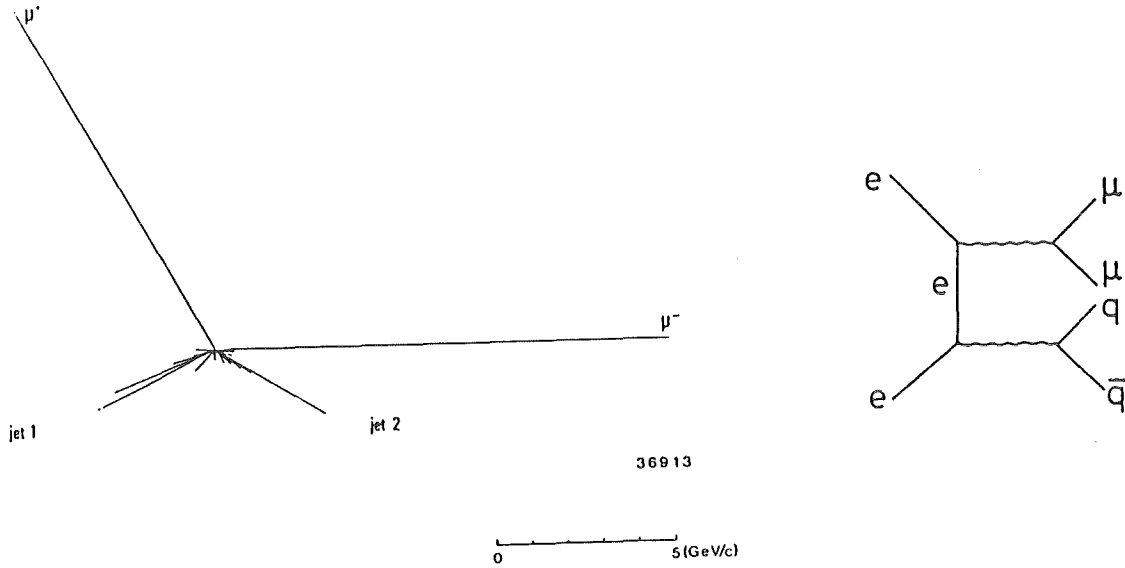


Figure 24: (a): momentum diagram of the dimuon event in the $\mu^+\mu^-$ plane
 (b): Feynman diagram for $e^+e^- \rightarrow \gamma^*\gamma^* \rightarrow \mu^+\mu^-q\bar{q}$.

- little or no missing energy ($.5 \pm 4$ GeV)
- high and similar μ momenta of $\sim 1/2 E_{beam}$ ($p_{\mu^+} = 11.0 \pm 2.5 GeV$, $p_{\mu^-} = 12.6 \pm 3.2 GeV$)
- the extreme planarity of the event ($\langle p_{t,out} \rangle$ of the hadrons w.r.t. the $\mu^+\mu^-$ plane is only 270 MeV)
- high and similar μ -jet masses close to $\sqrt{s}/2$ ($m_{\mu-jet1} = 22.5 \pm 1.6$, $m_{\mu-jet2} = 19.4 \pm 1.3$)

These features are suggestive of the pair production just above threshold (i.e. almost at rest) of a heavy object decaying back to back into a muon and a jet.

The most likely conventional source for such an event topology is α^4 QED pair production of two off shell photons decaying into $\mu^+\mu^-$ and $q\bar{q}$ (Fig. 24 b). The probability for QED to produce $\mu\mu$ and $q\bar{q}$ masses as high or higher than the observed ones was estimated to be $P_{QED} = 3 \cdot 10^{-4}$ based on a data sample of $4 pb^{-1}$. This estimate does not take into account the planarity of the event. However, since then no further event of this type was observed by any of the PETRA experiments. Combining the data samples at $\sqrt{s} \sim 44$ GeV and $\sqrt{s} \sim 35$ GeV (no threshold effect is involved in the QED process) of all 4 PETRA experiments the probability to observe such an event from QED rises to ~ 3 %.

4.3.2 Leptoquark searches

If leptons were built from coloured preons one would expect colour octet lepton states and colour triplet leptoquarks. These objects could be a candidate for a particle decaying into lepton and jet. This interpretation of the CELLO dimuon event is discussed in Refs. [39,40]. Leptoquark masses are expected to be of the order of the compositeness scale, i.e. above a few TeV. In Ref. [40], however, the possibility of a light spinless leptoquark goldstone boson is discussed. In this model three light leptoquark bosons of charge $2/3$ are expected, one for each family:

$$\begin{aligned} \chi_1 &\rightarrow u \bar{\nu}_e \text{ or } d e^+ \\ \chi_2 &\rightarrow c \bar{\nu}_\mu \text{ or } s \mu^+ \\ \chi_3 &\rightarrow t \bar{\nu}_\tau \text{ or } b \tau^+ \end{aligned}$$

These particles could be pair produced in e^+e^- annihilation with a cross section

$$\sigma(e^+e^- \rightarrow \chi_i\bar{\chi}_i) = 3Q^2\frac{1}{4}\beta^3\sigma_{\mu\mu}.$$

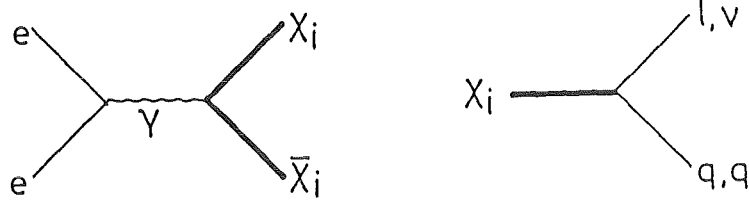


Figure 25: Feynman diagrams for leptoquark pair production and decay

The CELLO dimuon event is a natural candidate for pair production and muonic decay of a second generation leptoquark with a mass of ~ 20 GeV. To further investigate this possibility, CELLO [41] and JADE [42] made a systematic search for all three decay signatures of a second generation leptoquark (Fig. 26)

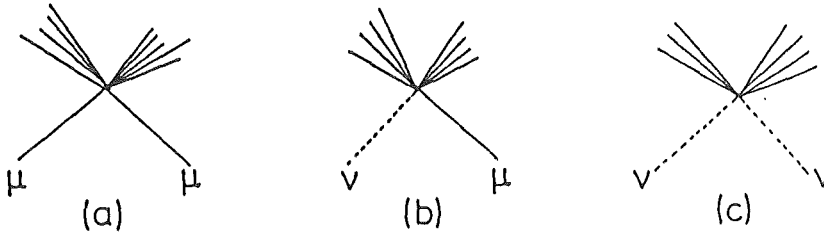


Figure 26: Signatures for pair production and decay of a second generation leptoquark: $\mu\mu jj$ (a), $\mu jj p_t$ (b), and $jj p_t$ (c)

The only unknowns in such a search are the leptoquark mass and its relative branching ratio into $e\bar{\nu}_\mu$ compared to $s\mu^+$. CELLO (JADE) observe 1(1), 0(1), and 2(0) events for the topologies $\mu\mu jj$, $\mu jj p_t$, and $jj p_t$ (see Fig. 26) respectively. Except for the CELLO dimuon event these candidates are compatible with known background sources. Fig. 27 shows the excluded leptoquark masses as a function of the muonic branching fraction. This analysis makes the leptoquark interpretation of the CELLO event unlikely, although it is interesting to note that it can not be completely excluded (see Fig. 27). However, leptoquarks of mass ~ 20 GeV should be produced sufficiently copiously in high energy $p\bar{p}$ collisions to check this hypothesis at the CERN $Spp\bar{S}$ collider.

5 Summary

Recent results on new particle searches at PETRA were reviewed. No evidence was found for new heavy leptons, neither charged nor neutral. Improved limits on mass and coupling of a heavy neutrino were shown.

Searches were made for the supersymmetric signatures

- acoplanar lepton, photon, and jet pairs
- single leptons, single photons, and single jets
- an excess of spherical events.

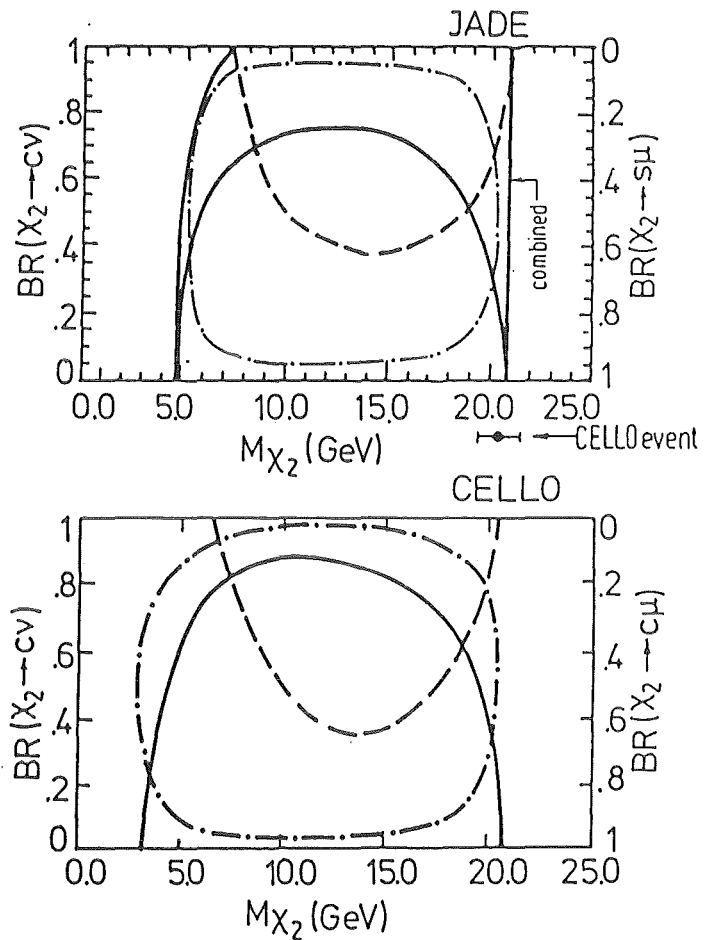


Figure 27: Excluded second generation leptoquark masses as function of the muonic branching ratio. Also indicated is the observed μ - jet mass of the CELLO dimuon event ($20.5 \pm 1.0 \text{ GeV}$).

No unexpected signal was observed in any of these signatures and improved mass limits on scalar electrons, photinos, gauginos, and higgsinos were obtained.

Searches for excited leptons of the electron, muon, and tau type were negative. A systematic search for light leptoquark scalar bosons makes the leptoquark interpretation of the CELLO dimuon event unlikely.

Acknowledgements

I wish to thank my colleagues at PETRA and CELLO for explaining me their latest results. I am grateful to Wim de Boer, John Field, and Eduardo Ros for reading the manuscript.

References

- [1] S. Komamiya, talk at the Int. Symp. on Lepton and Photon Int. at High Energies, Kyoto, Japan (1985), Heidelberg preprint HD-PY 86/01
J. Haissinski, talk at the XVI symposium on Multiparticle Dynamics, Kiryat-Anavim, Israel (1985), Orsay preprint LAL 85/32
- [2] CELLO coll, private communication
- [3] JADE coll, private communication
- [4] MARK-J coll, B. Adeva et al, Phys. Report 109(1984), 131
and A. Böhm, Proc. of the XXth Rencontre de Moriond, Les Arcs, 2(1985), 141
- [5] Proceedings of the VIth Moriond Workshop 'Massive Neutrinos in Particle Physics and Astrophysics', Tignes, France, (1986)
- [6] R. Aleksan, talk at the VIth Moriond Workshop 'Massive Neutrinos in Particle Physics and Astrophysics', Tignes, France, (1986), Saclay preprint DPhPE 86-08
- [7] G.J. Feldman, SLAC preprints SLAC-PUB-3684 and SLAC-PUB-3822,
C. Wendt et al., to be published
- [8] Kr.A. Gol'fan, E.P. Likhtman, JETP Lett. 13(1971),323
J. Wess, B. Zumino, Nucl. Phys. B70(1974),39
P. Fayet, S. Ferrara, Phys. Rep. 32C(1977), 249
- [9] J. Ellis and J.S. Hagelin, Nucl. Phys. B238(1984), 453
- [10] P. Fayet in "Unification of the Fundamental Particle Interactions", eds. S. Ferrara, J. Ellis, and P. Van Nieuwenhuizen (Plenum Press, N.Y., 1980), p. 587
- [11] N. Cabibbo, G.R. Farrar, and L. Maiani, Phys. Lett. 105B(1981),155
- [12] H. Komatsu and J. Kubo, Phys. Lett. 157B(1985), 90
- [13] G.L. Kane, this conference
- [14] CELLO coll., H.J. Behrend et al., *Search for Supersymmetric Particles at PETRA*, to be published
- [15] JADE coll., W. Bartel et al., Phys. Lett. 139B(1984),327 and S. Komamiya, private communication
- [16] MARK J coll., B. Adeva et al., Phys. Lett. 152B(1985),439
- [17] TASSO coll., M. Althoff et al., Z. Phys. C26(1984), 337
- [18] JADE coll., W. Bartel et al., DESY 84-112(1984)
- [19] TASSO coll., R. Brandelik et al., Phys Lett. 117B(1982), 365
- [20] CELLO coll., H.J. Behrend et al., DESY 86-50
- [21] ASP coll., G. Bartha et al., Phys. Rev. Lett. 56(1986), 685
- [22] M. Jonker, this conference
- [23] L.E Ibanez and C. Lopez, Nucl. Phys. B233(1984),511
J.S. Hagelin, G.L. Kane, and S. Raby, Nucl. Phys. B241(1984),638

- [24] MARK-J coll., B. Adeva et al., Phys. Rev. Lett. 53(1984),1806
- [25] JADE coll., W. Bartel et al., Phys. Lett. 146B(1984),126
- [26] JADE coll., W. Bartel et al., Z. Phys. C(1985),505
- [27] J. Ellis et al., Phys. Lett. 132B(1983),436
- [28] J.M. Frere and G.L. Kane, Nucl. Phys. B223(1983),331
- [29] E.J. Eichten, K.D. Lane, and M.E. Peskin, Phys Rev. Lett. 50(1983), 811
- [30] CELLO coll, private communication
- [31] JADE coll., W. Bartel et al, Z. Physik C19(1983), 197 and private communication
- [32] MARK-J coll., private communication
- [33] PLUTO coll., C. Berger et al., Z. Physik C27(1985), 341
- [34] TASSO coll., M. Althoff et al., Z. Physik C22(1984), 13
- [35] CELLO coll., H.J. Behrend et al., Phys. Lett. 168B(1986), 420
- [36] JADE coll., W. Bartel et al., DESY preprint 86-023(1986)
- [37] A. Courau and P. Kessler, LAL 85-01(1985)
- [38] CELLO coll., H.J. Behrend et al., Phys. Lett. 141B(1984), 145
- [39] R.N. Mohapatra, G. Segre, and L Wolfenstein, Phys. Lett. 145B(1984), 433
- [40] B. and F. Schrempp, Phys. Lett. 153B(1985), 101
- [41] CELLO collaboration, private communication
- [42] M. Kuhlen, private communication